Bull. Disas. Prev. Res. Inst., Kyoto Univ., Vol. 19, Part 2, No. 157, Nov. 1969

The Characteristics of Vibrations Produced by SH Type Torque in Multi-Layered Elastic Ground

By Michiyasu SHIMA and Kojiro IRIKURA

Abstract

The vibrational characteristics of multi-layered elastic ground are theoretically investigated in the case of the stationary harmonic vibration of the surface of the ground. As the first step we treat the vibration generated by SH torque that emits the pure SH torque wave of axial symmetry with respect to the vertical axis.

Integral expressions for the displacement fields are derived by using a technique applied first by N. A. Haskell to seismological problems. These expressions are transformed to complex integrals on the complex plane for ease of computation. As the points of computation of the displacement are near the origin, the branch line integrals become comparable with the contribution from the pole.

The numerical results are compared with the spectra in a case where an infinite train of harmonic plane waves is vertically transmitted to the surface layers. When the depth of the points is several times as large as the thickness of the surface layer, the peak and dip of the spectral curve approximately agree with those in the incidence of SH plane waves.

1. Introduction

It has gradually been clarified by many researchers that the vibrational characteristics of the ground in an earthquake depend on the structure of the ground. The characteristics of the ground are generally obtained from the results of the Fourier analyses of seismic waves recorded during natural earthquakes. However, it may not safely be said that they are determined only by the structure of the surface layers, since the frequency characteristics of the origin and the path through the crust influence the characteristics of the ground surface. If simultaneous measurements are made at the surface and points more than 100m below the bottom boundary plane, the characteristics of the structure of the ground can be extracted. However, it is very difficult to obtain them.

Waves produced by artificial oscillation may be suitable for known incident waves. A shaking machine with a range of frequency similar to that of earthquakes is an example of this, and it is often used to investigate the vibrational characteristics of various structures. In order to generate waves corresponding to seismic waves incident upwards, we must set the shaking machine underground, but this is very difficult. According to the reciprocity theorem, it is clarified that the same ocsillation as in the above case is obtained for the same shaking, even if the position of the source and the receiver is exchanged. Thus, in order to obtain the vibrational characteristics at the ground surface we may set the shaking machine on the surface and the seismometers underground.

In order to clarify the relations between the vibrational characteristics of the ground surface caused by upward incident plane waves and those caused by the incidence of spherical waves generated from a point source, we investigated the characteristics of the vibration of an elastic medium generated by horizontal (SH) torque source on the surface, when the elastic isotropic solid half space is composed of homogeneous layers with plane parallel boundaries.

Problems of elastic waves in a layered medium have been investigated in detail for a long time, mainly to clarify the phenomena of the propagation of surface waves and of dispersion[2]. These investigations were mainly directed to the behaviour of points distant from the source, and the features of waves near the source have hardly been investigated at all, because the perfect formation of the surface waves is distant from the source and the numerical calculation of the displacement near the source is difficult.

The vibrational characteristics in the case of the vertical incidence of plane waves correspond to that of the point beneath or near the source. Thus, we should investigate the frequency characteristics of the displacement near the SH torque source in order to find out the vibrational characteristics of the ground surface corresponding to the part of S waves in natural earthquakes. As the first step, we treated the waves which are emitted symmetrically with respect to the vertical axis from the SH torque source.

Integral expressions for the displacement were derived by using a technique applied by N. A. Haskell to seismological problems[3],[4]. That is, the integrand is composed of the product of Haskell's layer matrix for each layer and the factor expressing the characteristics of the source. These integral expressions are transformed to the integrals on the complex plane, and since the point of calculation is near the source, the contribution from the branch line integral is comparable with that from the pole.

2. Wave Equation and Formulation by Matrix

We consider a semi-infinite elastic medium made up of n parallel solid homogeneous isotropic layers as in Fig. 1 and a point source of SH torque type in the medium. Then, when the source oscillates harmonically, the spatially dependent factor $\bar{v}_j(r, z)$ of the azimuthal displacement $\bar{v}_j(r, z)e^{i\omega t}$ in each layer can be expressed by potential as $\bar{\chi}_j(r, z)$ follows:-

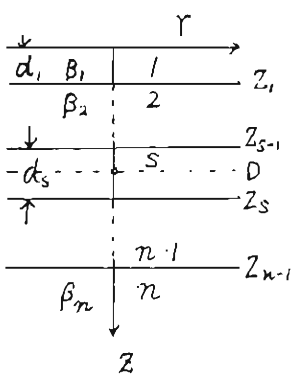

Fig. 1

$$\bar{v}_j(r, z) = -\frac{\partial \bar{\chi}_j(r, z)}{\partial r} \tag{1}$$

The wave equation is satisfied if $\bar{\chi}_j(r, z)$ is the solution of

$$\nabla^2\bar{\chi}_j(r, z) = -k_j^2\bar{\chi}_j(r, z) \tag{2}$$

As the source is the SH type with axial symmetry in this case, the displacement is only the azimuthal component and is independent of θ.

The azimuthal tangential stress is

$$\bar{p}^{\theta z}{}_j(r, z) = -\mu_j\frac{\partial^2\bar{\chi}_j(r, z)}{\partial r\partial z} \tag{3}$$

We now express $\bar{\chi}_j(r, z)$ by integral expression as follows:-

$$\bar{\chi}_j(r, z) = \int_0^\infty \chi_j(z)J_0(kr)dk \tag{4}$$

Then we substitute (4) into equation (1), (3). Equating integrals, we obtain

$$\begin{aligned}\bar{v}_j(r,z)&=\int_0^\infty\left\{-\chi_j(z)\frac{dJ_0(kr)}{dr}\right\}dk\equiv\int_0^\infty\frac{i\dot{v}_j(z)}{kc}\frac{dJ_0(kr)}{d(kr)}dk\\ \bar{p}_{\theta z_j}(r,z)&=\int_0^\infty\left\{-\mu_j\frac{d\chi_j(z)}{dz}\frac{dJ_0(kr)}{d(kr)}\right\}dk\equiv\int_0^\infty\left\{-\tau_j(z)\frac{dJ_0(kr)}{d(kr)}\right\}dk\end{aligned}\tag{5}$$

where we have used the following relations

$$\frac{d^2\chi_j(z)}{dz^2}=(k^2-k_j^2)\chi_j(z)\tag{6}$$

At the interface between two layers, we impose the boundary condition of continuity of displacement and stress. This continuity at $j-1$ interface between layers $j-1$ and j can be expressed as follows.

$$\begin{bmatrix}\dfrac{\dot{v}_j(z_{j-1})}{c}\\ \tau_j(z_{j-1})\end{bmatrix}=\begin{bmatrix}\dfrac{\dot{v}_{j-1}(z_{j-1})}{c}\\ \tau_{j-1}(z_{j-1})\end{bmatrix}\tag{7}$$

For layers not containing a source, we use for $\chi_j(z)$ the general solutions of equation (6)

$$\chi_j(z)=\bar{\epsilon}_j'e^{-i\gamma_j z}+\bar{\epsilon}_j''e^{i\gamma_j z}\tag{8}$$

Defining

$$\epsilon_j'=\bar{\epsilon}_j'ke^{-i\gamma_j z_{j-1}},\qquad \epsilon_j''=\bar{\epsilon}_j''ke^{i\gamma_j z_{j-1}}\tag{9}$$

and substitute (8) into equation (5), we obtain

$$\begin{aligned}\frac{\dot{v}_j(z)}{c}&=(\epsilon_j'+\epsilon_j'')ik\cos\{\gamma_j(z-z_{j-1})\}+(\epsilon_j'-\epsilon_j'')k\sin\{\gamma_j(z-z_{j-1})\}\\ \tau_j(z)&=-(\epsilon_j'+\epsilon_j'')\mu_j\gamma_j\sin\{\gamma_j(z-z_{j-1})\}-(\epsilon_j'-\epsilon_j'')i\mu_j\gamma_j\cos\{\gamma_j(z-z_{j-1})\}\end{aligned}\tag{10}$$

Evaluating equation (10) for j-th layer at $z=z_{j-1}$, we obtain

$$\begin{bmatrix}\dfrac{\dot{v}_j(z_{j-1})}{c}\\ \tau_j(z_{j-1})\end{bmatrix}=E_j\begin{bmatrix}\epsilon_j'+\epsilon_j''\\ \epsilon_j'-\epsilon_j''\end{bmatrix}\tag{11}$$

or

$$\begin{aligned}\begin{bmatrix}\epsilon_j'+\epsilon_j''\\ \epsilon_j'-\epsilon_j''\end{bmatrix}&=E_j^{-1}\begin{bmatrix}\dfrac{\dot{v}_j(z_{j-1})}{c}\\ \tau_j(z_{j-1})\end{bmatrix}\\ E_j^{-1}&=\begin{pmatrix}(ik)^{-1}&0\\0&-(ik\mu_j\beta_j)^{-1}\end{pmatrix}\end{aligned}\tag{12}$$

and evaluating (10) at $z=z_j$, we can eliminate the coefficients $(\epsilon_j'+\epsilon_j'')$ and $(\epsilon_j'-\epsilon_j'')$, and obtain the Haskell matrix.

$$\begin{bmatrix}\dfrac{\dot{v}_j(z_j)}{c}\\ \tau_j(z_j)\end{bmatrix}=a_j\begin{bmatrix}\dfrac{\dot{v}_j(z_{j-1})}{c}\\ \tau_j(z_{j-1})\end{bmatrix}\tag{13}$$

$$\begin{aligned}a_j&=\begin{pmatrix}\cos Q_j&\dfrac{ik\sin Q_j}{\mu_j\gamma_j}\\ \dfrac{i\mu_j\gamma_j\sin Q_j}{k}&\cos Q_j\end{pmatrix}\\ Q_j&=\gamma_j d_j\end{aligned}\tag{14}$$

For source layer s, we use a point source located at D, $(z_s<D<z_{s-1})$ such that the z dependent integrands of the source potential are the solution of equation (6) everywhere in s continuous with continuous derivatives except at D or

$$\chi_{S0}(z) = \begin{cases} S_0^+ e^{-i\gamma_S(z-D)} \ ; & z > D \\ S_0^- e^{-i\gamma_S(D-z)} \ ; & z < D \end{cases} \tag{15}$$

Combining (15) with the solution of equation (6), the general potential for the source layer is

$$\begin{aligned} \chi_S(z) &= \bar{\epsilon}_{S1}' e^{-i\gamma_S z} + \bar{\epsilon}_{S1}'' e^{i\gamma_S z} \ ; & z < D \\ \chi_S(z) &= \bar{\epsilon}_{S2}' e^{-i\gamma_S z} + \bar{\epsilon}_{S2}'' e^{i\gamma_S z} \ ; & z > D \end{aligned} \tag{16}$$

where

$$\begin{aligned} \bar{\epsilon}_{S1}' &= \bar{\epsilon}_S', & \bar{\epsilon}_{S1}'' &= \bar{\epsilon}_S'' + S_0^- e^{-i\gamma_S D} \\ \bar{\epsilon}_{S2}' &= \bar{\epsilon}_S' + S_0^+ e^{i\gamma_S D}, & \bar{\epsilon}_{S2}'' &= \bar{\epsilon}_S'' \end{aligned} \tag{17}$$

$\bar{\epsilon}_{S1}'$, $\bar{\epsilon}_{S1}''$, $\bar{\epsilon}_{S2}'$, $\bar{\epsilon}_{S2}''$ are those of the same character as the coefficients for the layers not containing the source and (16) is the same form as (8). Therefore, using the same as the procedures for the layers not containing the source, we obtain the following matrix relations for the source layers

$$\begin{aligned} \begin{bmatrix} \dfrac{\dot{v}_{S1}(D)}{c} \\ \tau_{S1}(D) \end{bmatrix} &= a_{S1} \begin{bmatrix} \dfrac{\dot{v}_{S1}(z_{S-1})}{c} \\ \tau_{S-1}(z_{S-1}) \end{bmatrix} \\ \begin{bmatrix} \dfrac{\dot{v}_{S2}(z_S)}{c} \\ \tau_{S2}(z_S) \end{bmatrix} &= a_{S2} \begin{bmatrix} \dfrac{\dot{v}_{S2}(D)}{c} \\ \tau_{S2}(D) \end{bmatrix} \end{aligned} \tag{18}$$

$$a_{Sl} = \begin{pmatrix} \cos Q_{Sl} & \dfrac{ik \sin Q_{Sl}}{\mu_S \gamma_S} \\ \dfrac{i\mu_S \gamma_S \sin Q_{Sl}}{k} & \cos Q_{Sl} \end{pmatrix} \tag{19}$$

$$Q_{S1} = \gamma_S (D - z_{S-1}) \qquad Q_{S2} = \gamma_S (z_S - D)$$

And we have

$$\begin{bmatrix} \dfrac{\dot{v}_{S2}(D)}{c} \\ \tau_{S2}(D) \end{bmatrix} = \begin{bmatrix} \dfrac{\dot{v}_{S1}(D)}{c} \\ \tau_{S1}(D) \end{bmatrix} + \begin{bmatrix} \delta\left(\dfrac{\dot{v}_S}{c}\right) \\ \delta\tau_S \end{bmatrix} \tag{20}$$

where from (5) and (16)

$$\begin{aligned} \delta\left(\frac{\dot{v}_S}{c}\right) &= ik^2 (S_0^+ - S_0^-) \\ \delta\tau_S &= -ik\mu_S \gamma_S (S_0^+ + S_0^-) \end{aligned} \tag{21}$$

3. Solutions for the SH Torque Source

Now according to the consideration in the introduction, we set the source on the surface and investigate the frequency characteristics of the displacement in the layers. For simplicity, we take the SH torque source which radiates spherical waves and use the following potential

$$\bar{\chi}_0(r, z) = \frac{e^{ik_1\sqrt{r^2+z^2}}}{\sqrt{r^2+z^2}} \tag{22}$$

By means of the Sommerfeld integral, we can express (22) as

$$\bar{\chi}_0(r, z) = \int_0^\infty S_0^{\pm} e^{-i\gamma_1 |z-D|} J_0(kr) dk \tag{23}$$

$$S_0^+ = S_0^- = \frac{-ik}{\sqrt{k_1^2 - k^2}}$$

By (21)

$$\delta\left(\frac{\dot{v}_1}{c}\right)=0, \qquad \delta\tau_1=-2\mu_1 k^2 \tag{24}$$

As the source is on the surface

$$a_{s1}=\begin{pmatrix}1 & 0\\ 0 & 1\end{pmatrix}, \qquad \tau_{s1}(D)=0$$

For the three layered medium, from the boundary condition (17), (18) and (20), we have the following expressions for the displacements in the first and second layers

$$\begin{bmatrix}\dfrac{\dot{v}_2(z_2)}{c}\\ \tau_2(z_2)\end{bmatrix}=a_2a_1\begin{bmatrix}\dfrac{\dot{v}_{12}(D)}{c}\\ \tau_{12}(D)\end{bmatrix}=a_2a_1\begin{bmatrix}\dfrac{\dot{v}_1(0)}{c}\\ \delta\tau_1\end{bmatrix} \tag{25}$$

From equation (12), we have for the half space or bottom layer :-

$$\begin{bmatrix}\epsilon_3'+\epsilon_3''\\ \epsilon_3'-\epsilon_3''\end{bmatrix}=E_3^{-1}\begin{bmatrix}\dfrac{\dot{v}_3(z_2)}{c}\\ \tau_3(z_2)\end{bmatrix}=E_3^{-1}\begin{bmatrix}\dfrac{\dot{v}_2(z_2)}{c}\\ \tau_2(z_2)\end{bmatrix} \tag{26}$$

As a boundary condition for the half-space, we require that the coefficients ϵ_3'' vanish. Because when the source is on the surface, there is no radiation from infinity for greater than the half-space S wave velocity, displacement and stress remain finite for c less than the S wave velocity as the depth becomes infinite. With this boundary condition, (26) reduces to

$$\begin{bmatrix}\epsilon_3'\\ \epsilon_3'\end{bmatrix}=E_3^{-1}\begin{bmatrix}\dfrac{\dot{v}_2(z_2)}{c}\\ \tau_2(z_2)\end{bmatrix} \tag{27}$$

Substituting (25) into (27), we have

$$\begin{bmatrix}\epsilon_3'\\ \epsilon_3'\end{bmatrix}=E_3^{-1}a_2a_1\begin{bmatrix}\dfrac{\dot{v}_1(0)}{c}\\ \delta\tau_1\end{bmatrix}\equiv J\begin{bmatrix}\dfrac{\dot{v}_1(0)}{c}\\ \delta\tau_1\end{bmatrix} \tag{28}$$

Eliminating ϵ_3' from (28) yields

$$\frac{\dot{v}_1(0)}{c}=\frac{J_{22}-J_{12}}{J_{11}-J_{21}}\delta\tau_1 \tag{29}$$

Substituting (29) into (25), we have

$$\frac{\dot{v}_1(z)}{c}=\frac{J_{22}-J_{12}}{J_{11}-J_{21}}[a_1(z)]_{11}\delta\tau_1+[a_1(z)]_{12}\delta\tau_1 \tag{30}$$

$$\frac{\dot{v}_2(z)}{c}=\frac{J_{22}-J_{12}}{J_{11}-J_{21}}[a_2(z)a_1]_{11}\delta\tau_1+[a_2(z)a_1]_{12}\delta\tau_1 \tag{31}$$

where $a_1(z)$ and $a_2(z)$ are given by

$$a_1(z)=\begin{pmatrix}\cos\gamma_1 z & -\dfrac{ik\sin\gamma_1 z}{\mu_1\gamma_1}\\ \dfrac{i\mu_1\gamma_1\sin\gamma_1 z}{k} & \cos\gamma_1 z\end{pmatrix}$$

$$a_2(z)=\begin{pmatrix}\cos\gamma_2(z-d_1) & \dfrac{ik\sin\gamma_2(z-d_1)}{\mu_2\gamma_2}\\ \dfrac{i\mu_2\gamma_2\sin\gamma_2(z-d_1)}{k} & \cos\gamma_2(z-d_1)\end{pmatrix} \tag{32}$$

For the half-space, setting $\epsilon_3''=0$ in equation (10) for $j=3$, evaluating $\dot{v}_3/c$ and τ_3 at $z=z$, and $z=z_2$, and eliminating ϵ_3' from those equations, we obtain

$$\begin{bmatrix}\dfrac{\dot{v}_3(z)}{c}\\ \tau_3(z)\end{bmatrix}=\{\cos\gamma_3(z-d_1-d_2)-i\sin\gamma_3(z-d_1-d_3)\}\begin{bmatrix}\dfrac{\dot{v}_3(z_2)}{c}\\ \tau_3(z_2)\end{bmatrix} \tag{33}$$

Therefore, substituting (31) into (33), we have

$$\frac{\dot{v}_3(z)}{c}=\{\cos\gamma_3(z-d_1-d_2)-i\sin\gamma_3(z-d_1-d_2)\}$$
$$\times\left[\frac{J_{22}-J_{12}}{J_{11}-J_{21}}[a_2a_1]_{11}+[a_2a_1]_{12}\right]\delta\tau_1 \tag{34}$$

Substituting (30), (31), (34) into (5), we have the integral expressions for the displacements in each layer. The sign of γ_j is determined by the condition $I_m\gamma_j\leq 0$, since with this choice infinite value of the displacement as $z\to\infty$ is avoided. On this leaf of the Riemann surface

$$\gamma_j=\sqrt{k_j^2-k^2}=-i\sqrt{k^2-k_j^2}\equiv -i\bar{\gamma}_j \tag{35}$$

Then

$k_2<k<k_1$:

$$J_{11}-J_{21}=\frac{\cos Q_1\cosh Q_2-\left(\frac{\mu_1\gamma_1}{\mu_3\bar{\gamma}_3}\right)\sin Q_1\cosh Q_2+\left(\frac{\mu_2\bar{\gamma}_2}{\mu_3\bar{\gamma}_3}\right)\cos Q_1\sinh Q_2-\left(\frac{\mu_1\gamma_1}{\mu_2\bar{\gamma}_2}\right)\sin Q_1\sinh Q_2}{ik}$$

$$J_{22}-J_{12}=\frac{\cos Q_1\cosh Q_2+\left(\frac{\mu_3\bar{\gamma}_3}{\mu_1\gamma_1}\right)\sin Q_1\cosh Q_2+\left(\frac{\mu_3\bar{\gamma}_3}{\mu_2\bar{\gamma}_2}\right)\cos Q_1\sinh Q_2+\left(\frac{\mu_2\bar{\gamma}_2}{\mu_1\gamma_1}\right)\sin Q_1\sinh Q_2}{-\mu_3\bar{\gamma}_3}$$

$$[a_2a_1]_{11}=\cos Q_1\cosh Q_2-\left(\frac{\mu_1\gamma_1}{\mu_2\bar{\gamma}_2}\right)\sin Q_1\sinh Q_2$$
$$[a_2a_1]_{12}=ik\left\{\frac{\cos Q_1\sinh Q_2}{\mu_2\bar{\gamma}_2}+\frac{\sin Q_1\cosh Q_2}{\mu_1\gamma_1}\right\} \tag{36}$$

$k_3<k<k_2$:

$$J_{11}-J_{21}=\frac{\cos Q_1\cos Q_2-\left(\frac{\mu_1\gamma_1}{\mu_3\bar{\gamma}_3}\right)\sin Q_1\cos Q_2-\left(\frac{\mu_2\gamma_2}{\mu_3\bar{\gamma}_3}\right)\cos Q_1\sin Q_2-\left(\frac{\mu_1\gamma_1}{\mu_2\gamma_2}\right)\sin Q_1\sin Q_2}{ik}$$

$$J_{22}-J_{12}=\frac{\cos Q_1\cos Q_2+\left(\frac{\mu_3\bar{\gamma}_3}{\mu_1\gamma_1}\right)\sin Q_1\cos Q_2+\left(\frac{\mu_3\bar{\gamma}_3}{\mu_2\gamma_2}\right)\cos Q_1\sin Q_2-\left(\frac{\mu_2\gamma_2}{\mu_1\gamma_1}\right)\sin Q_1\sin Q_2}{-\mu_3\bar{\gamma}_3}$$

$$[a_2a_1]_{11}=\cos Q_1\cos Q_2-\left(\frac{\mu_1\gamma_1}{\mu_2\gamma_2}\right)\sin Q_1\sin Q_2$$
$$[a_2a_1]_{12}=ik\left\{\frac{\cos Q_1\sin Q_2}{\mu_2\gamma_2}+\frac{\sin Q_1\cos Q_2}{\mu_1\gamma_1}\right\} \tag{37}$$

$k<k_3$:

$$J_{11}-J_{21}=\frac{\cos Q_1\cos Q_2-\left(\frac{\mu_1\gamma_1}{\mu_2\gamma_2}\right)\sin Q_1\sin Q_2+i\left[\left(\frac{\mu_2\gamma_2}{\mu_3\gamma_3}\right)\cos Q_1\sin Q_2+\right.}{ik}$$

$$\left(\frac{\mu_1\gamma_1}{\mu_3\gamma_3}\right)\sin Q_1 \cos Q_2\Big\}$$

$$J_{22}-J_{12}=\frac{\left(\frac{\mu_3\gamma_3}{\mu_1\gamma_1}\right)\sin Q_1 \cos Q_2+\left(\frac{\mu_3\gamma_3}{\mu_2\gamma_2}\right)\cos Q_1 \sin Q_2+i\{-\cos Q_1 \cos Q_2+}{-\mu_3\gamma_3}$$

$$\left(\frac{\mu_2\gamma_2}{\mu_1\gamma_1}\right)\sin Q_1 \sin Q_2\}$$

$$[a_2a_1]_{11}=\cos Q_1 \cos Q_2-\left(\frac{\mu_1\gamma_1}{\mu_2\gamma_2}\right)\sin Q_1 \sin Q_2$$

$$[a_2a_1]_{12}=ik\left\{\frac{\sin Q_1 \cos Q_2}{\mu_1\gamma_1}+\frac{\cos Q_1 \sin Q_2}{\mu_2\gamma_2}\right\} \tag{38}$$

4. Evaluation of Integrals

The displacements in each layer are given by

$$\bar{v}_j(r,z)=i\int_0^\infty \frac{\dot{v}_j(z)}{ck}\frac{dJ_0(kr)}{d(kr)}dk=-i\int_0^\infty \frac{\dot{v}_j(z)}{ck}J_1(kr)dk\equiv$$

$$\int_0^\infty F_j(k,\gamma_3)J_1(kr)dk \tag{39}$$

where $F_j(k,\gamma_3)$ is the even valued function of k. Since $F_j(k,\gamma_3)$ is the even valued function of γ_1, γ_2, the corresponding branch points vanish. Only the branch point k_3 corresponding to the half space medium determines the Riemann surface. Thus the Riemann surface is two leaved, as represented in Figs. 2 and 3. As in Fig. 2, the cut given by the condition $I_m\gamma_3=0$ begins at k_3 runs

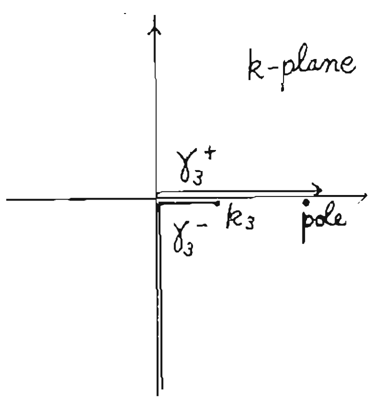

Fig. 2 Branch line and residues in k-plane.

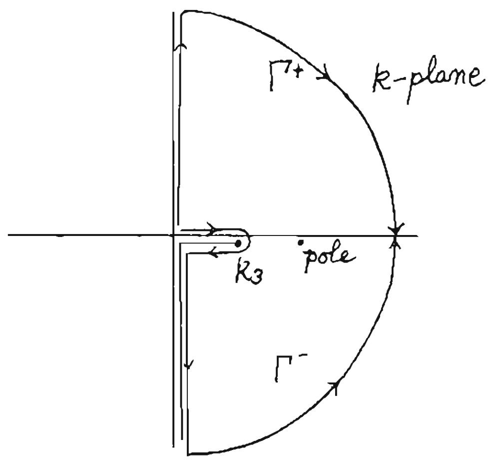

Fig. 3 Distortion of contour in k-plane.

to the origin along the real axis, and then goes to $-i\infty$ along the negative imaginary axis. The branch point k_3 is in the side of the fourth quadrant and the real poles of $F_j(k,\gamma_3)$ are on the upper leaf of the Riemann surface. It was shown that the complex poles are not located on the permissible sheet of the Riemann surface.

Expressing the $J_1(kr)$ by the Hankel functions of the first and the second kind, respectively, we have

$$\bar{v}_j(r,z)=\frac{1}{2}\int_0^\infty F_j(k,\gamma_3)H_1^{(1)}(kr)dk+\frac{1}{2}\int_0^\infty F_j(k,\gamma_3)H_1^{(2)}(kr)dk \tag{40}$$

Since we require the calculation of the displacements for a small value of r we cannot use the method of the steepest descent which is the usual one in the line integral. In order to calculate the integrals (40) easily, the first term of equation (40) along the real axis may be replaced by the integral along the path Γ^+ in Fig. 3 and the second term by the integral along the Γ^- using Cauchy's theorem. That is, the integrals become integrals along the imaginary axis, branch line integrals and the residues.

We shall denote by the symbols γ_3^+ in the first or γ_3^- in the fourth quadrant that $Re\gamma_3>0$ or $Re\gamma_3<0$, respectively. By use of the relation $H_1^{(1)}(kr)=H_1^{(2)}(kr)$, from (40), we have

$$\bar{v}_j(r,z)=\frac{1}{2}\Big[\int_0^{k_3}\{F_j(k,\gamma_3^+)-F_j(k,\gamma_3^-)\}H_1^{(2)}(kr)dk+\frac{2}{i\pi}\int_0^\infty\{F_j(i\tau,\gamma_3^+)-$$

$$F_j(i\tau,\gamma_3^-)\}K_1(\tau r)d\tau-2\pi i\sum\mathrm{Res}\{F_j(k,\gamma_3)\,H_1^{(2)}(kr)\}\Big] \tag{41}$$

$$F_3(k,\gamma_3^+)-F_3(k,\gamma_3^-)=i4\mu_1k^2\{AC\cos Q_3+(BC+D)\sin Q_3\} \tag{42}$$

$$A=\frac{ac+bd}{c^2+d^2},\qquad B=\frac{bc-ad}{c^2+d^2}$$

$$a=-\cos Q_1\cos Q_2+\left(\frac{\mu_2\gamma_2}{\mu_1\gamma_1}\right)\sin Q_1\sin Q_2$$

$$b=-\left(\frac{\mu_3\gamma_3}{\mu_1\gamma_1}\right)\sin Q_1\cos Q_2-\left(\frac{\mu_3\gamma_3}{\mu_2\gamma_2}\right)\cos Q_1\sin Q_2$$

$$c=\mu_3\gamma_3\{\cos Q_1\cos Q_2-\left(\frac{\mu_1\gamma_1}{\mu_2\gamma_2}\right)\sin Q_1\sin Q_2\} \tag{43}$$

$$d=\mu_1\gamma_1\sin Q_1\cos Q_2+\mu_2\gamma_2\cos Q_1\sin Q_2$$

$$C=\cos Q_1\cos Q_2-\left(\frac{\mu_1\gamma_1}{\mu_2\gamma_2}\right)\sin Q_1\sin Q_2$$

$$D=\sin Q_1\cos Q_2/\mu_1\gamma_1+\cos Q_1\sin Q_2/\mu_2\gamma_2$$

$$Q_1=\gamma_1d_1,\quad Q_2=\gamma_2d_2,\quad Q_3=\gamma_3(z-d_1-d_2)$$

For $F_2(k,\gamma_3^+)-F_2(k,\gamma_3^-)$, Q_2 and Q_3 are replaced by

$$Q_2=\gamma_2(z-d_1),\quad Q_3=0 \tag{44}$$

For $F_1(k,\gamma_3^+)-F_1(k,\gamma_3^-)$, Q_1, Q_2 and Q_3 are replaced by

$$Q_1=\gamma_1z,\quad Q_2=Q_3=0 \tag{45}$$

Though in integral (5), $H_1^{(2)}(kr)$ and $K_1(\tau r)$ and have their singular point at $k,\tau=0$, the integrands tend to zero for $k,\tau\to0$. Thus the integrands have no pole at $k=\tau=0$.

5. Results of the Calculation and Some Considerations

We show some results obtained from the numerical calculation of the frequency characteristics of the displacements for the various examples of the layered medium. The structures of the medium numerically calculated are similar to those of grounds in cities. That is, regarding S wave velocity, we take a set of 100m/s, 200m/s, 400m/s, in the first, second, and third layers, respectively, and a set of 100m/s, 300m/s, 600m/s. Regarding the thickness of the layers, the examples of $|\bar{v}_j(r, z)|$ which are calculated for the various sets of thicknesses of the layers are shown in Figs. 4-7. As the source is on the surface in this case and the frequency characteristics of the amplitude of displacement of the SH wave generated are flat, the frequency characteristics become flat as $r, z \to 0$. The point of calculation is not beneath the source, but is 5m horizontally from the source. Because when r is too near zero, the convergence of the calculation of the integral is not good, and generally, the location of the seismometer used in an observation is not beneath the shaking machine, but set several meters horizontally from it.

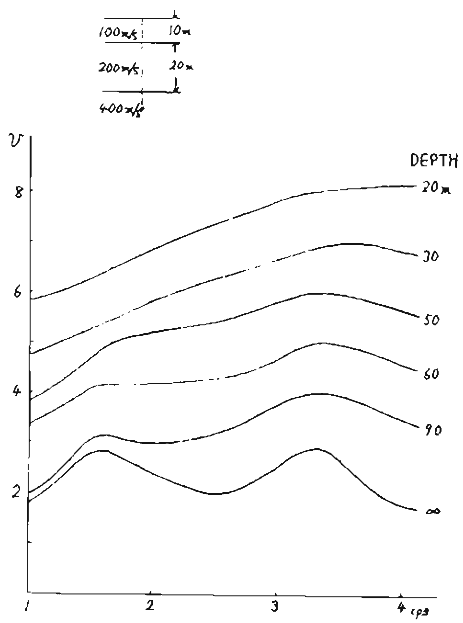

Fig. 4 Amplitudes of displacement versus frequency for several depths and SH plane wave.

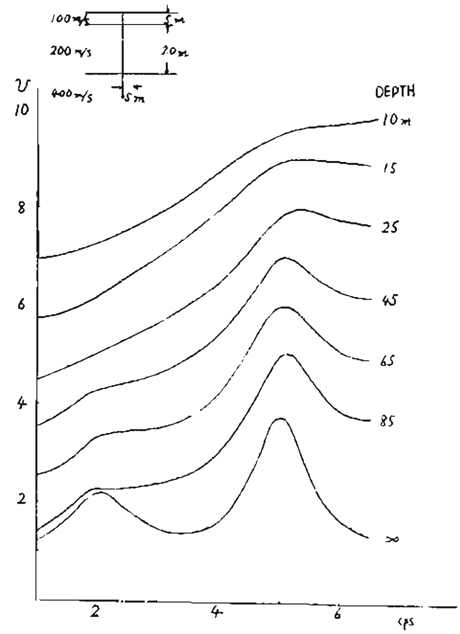

Fig. 5 Amplitudes of displacement versus frequency for several depths and SH plane wave.

For the source of the type of equation (2), the amplitude of displacement decreases fast as $z \to \infty$. Therefore, in the illustration, we normalize the amplitude curves at each depth, such that the maximum of the curves at each depth becomes the same value in spite of the depth. And we displace upwards in order the zero level of each curve, unit by unit. The lowest curve expresses the frequency characteristics of the displacement of the surface when a plane SH wave having frequency characteristics of constance regarding the displacement is incident on the bottom plane.[5]

In these figures, we expressed the frequency characteristics as those of the amplitude in the medium for the source on the surface. As, according to the reciprocity theorem in elastic theory, the same oscillation as in the above case is obtained for the same shaking when the positions of the source and the receiver are exchanged, the examples in these figures are equivalent to the results of

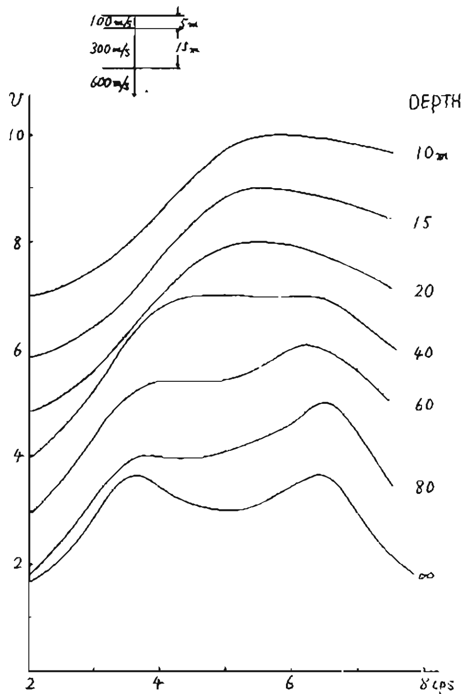

Fig. 6 Amplitudes of displacement versus frequency for several depths and SH plane wave.

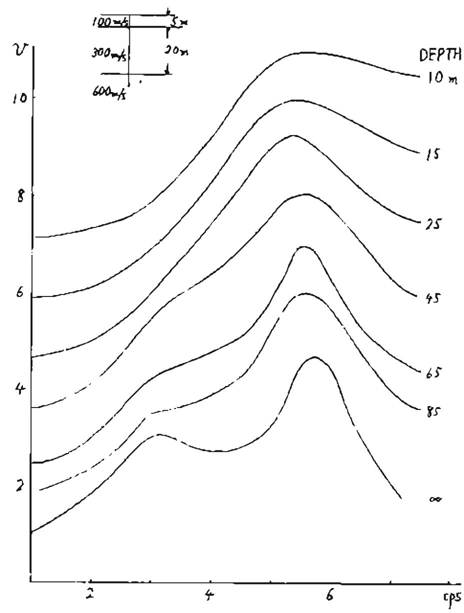

Fig. 7 Amplitudes of displacement versus frequency for several depths and SH plane wave.

the shaking of the underground points. For the range shown in the figures of the frequency, the curves have one peak and one ambiguious peak or a beginning point of the rapid decrease of displacement towards the lower frequency. The peak of the lower frequency of the two peaks in the four curves corresponding to the points of the bottom layer corresponds to the fundamental mode of the surface layer consisting of the two layers, and the peak of the higher frequency to the second mode. The feature of the fundamental mode in the curves of the displacements of the second layer almost disappears. Only the peak of the second mode appears in the curves. However, this peak also disappears in the curves of the first layer. In this manner, the vibrational characteristics of the layered medium gradually become evident with the depth of the point of the receiver.

Only the second mode appears in the curves of the second layer, which corresponds to the fundamental mode when the second and third layers may be regarded as the bottom layer. Thus, joining this with the results obtained from the calculation of the points in the bottom layer, it may be said that if we regard layers above the observation point as a surface layer, we can estimate the frequency of the fundamental mode for such a surface layer.

As is clear from the features, it is desirable that the receiving points be set as deep as possible. However, in practice we are forced to set the observation point shallowly for the sake of economy. If we measure the feature of the decrease of the displacement towards the lower frequency exactly, even with respect to the fundamental mode, we may find the frequency of the mode at the observation point shallow from the bottom plane.

References

1) Knopoff, L., and A. F. Gangi : Seismic Reciprccity, Geophysics, Vol. 24, 1959, pp. 681-691.
2) Ewing, W. M., W. S. Jardetzky, and F. Press : Elastic Waves in Layered Media, 1957, pp. 124-254.
3) Haskell, N. A. : The Dispersion of Surface Waves on Multilayered Media, Bull. Seis. Scc. Am., Vol. 43, 1953, pp. 17-34.
4) Harkrider, D. G. : Surface Waves in Multilayered Elastic Media 1., Bull. Seis. Soc. Am., Vol. 54, 1964, pp. 627-679.
5) Kanai, K. : Relation between the Amplitude of earthquake motions and the Nature of Surface Layer IV., Bull. Earthquake Research Institute, Tokyo Univ., Vol. 34., 1956, pp. 167-184.